Resonance in the response of the bacterial flagellar motor to thermal oscillations

Mahmut Demir and Hanna Salman

Phys. Rev. E **95**, 022419 — Published 28 February 2017

DOI: 10.1103/PhysRevE.95.022419

Resonance in the response of the bacterial flagellar-motor to thermal oscillations

Mahmut Demir[1,&] and Hanna Salman[1,2,*]

[1] Department of Physics and Astronomy, The Dietrich School of Arts and Sciences

[2] Department of Computational and Systems Biology, School of Medicine

University of Pittsburgh, Pittsburgh, PA

[&] Current address: Department of Molecular, Cellular and Developmental Biology, Yale University, New Haven, CT

[*] Correspondence should be addressed to hsalman@pitt.edu

Abstract

We have studied the dynamics of the *E. coli* flagellar motor's angular velocity in response to thermal oscillations. We find that the oscillations' amplitude of the motor's angular velocity exhibits resonance when the temperature is oscillated at frequencies around 4 Hz. This resonance appears to be due to the existence of a natural mode of oscillations in the state of the motor, specifically in the torque generated by the motor. Natural modes of oscillation in torque generation cannot result from random fluctuations in the state of the motor. Their presence points to the existence of a coupling mechanism between the magnitude of the torque generated by the motor and the rates of transition between the different states of the motor components responsible for torque generation. The results presented here are the first to show resonance response in torque generation to external perturbations. They are explained with a simple phenomenological model, which can help future studies identify the source of the feedback mechanism between the torque and the interactions responsible for its generation. It can also help us to quantitatively estimate the strength of these interactions and how they are affected by the magnitude of the torque they generate.

Introduction

Escherichia coli (*E. coli*), like many other microorganisms, swim in pursuit of environmental cues using long helical flagella. These flagella are rotated by a bi-directional rotary motor embedded in the cell wall known as the bacterial flagellar motor (BFM) [1]. The BFM is a complex machine consisting of many interacting components that work together in an orchestrated manner to rotate the bacterial flagella. There has been a great interest in understanding the operation mechanism of these motors as well as other rotary motors, such as the F-ATPase. This is due to the important role these motors play in the cell's life and function and as an example of an efficient biological machine that converts electrochemical energy into mechanical work. In the case of the BFM for example, the electrochemical energy is supplied by the proton motive force (PMF) which is a result of the electric potential and pH differences across the membrane [2]. The proton motive force generates a proton flux into the cell, which drives the motor's rotation.

The BFM is a tightly coupled stepper motor [3]. Its rotation is strictly coupled to the proton flux through its stator complexes [4], which consist of 2 subunits, MotA and MotB [5]. These complexes anchor to the peptidoglycan cell wall via their MotB subunits, while their MotA subunits span the cytoplasmic membrane forming channels for proton translocation [6–8]. The cytoplasmic domain of MotA contains two charged residues. These residues interact with five charged residues on the protein FliG that forms the cytoplasmic ring of the motor's rotor, to generate torque [9–13]. Torque is generated when the rotor is made to take a step by the translocation of 2 protons through a stator. In addition to the FliG proteins, the cytoplasmic ring of the rotor consists of two other proteins, FliM and FliN. Together, these proteins are believed to be responsible for switching the rotational direction of the rotor from its natural direction, counter clockwise (CCW), to clockwise (CW). The switch occurs upon binding of the cell's signal transduction network response regulator, CheY, in its phosphorylated state (CheY-P) to FliG. The binding of CheY-P is believed to stabilize a conformational state of FliG, which causes the rotor to rotate CW when pushed by the stators.

The structure of these fascinating motors, like many other biological machines, is not fixed and they exhibit wide variability in their content. Recently, it has been shown that the number of stators in the motor, changes as a function of the load on the motor [14], which is equivalent to the drag force resisting the motor's rotation. Since these machines operate in the low Reynolds

number regime the drag force is equal to the driving force and is proportional to the rotational speed: $F_d r = \tau \propto \eta v r$, where F_d is the drag force, τ is the driving torque of the motor, η is the medium's viscosity and $v = \omega r$, is the rotational speed of the motor, where ω is its angular velocity, and r is the radius of the load's rotation. This implies that the stator-rotor interaction is load-dependent and as a result torque-dependent. This feedback between the torque and the stator-rotor interaction is important to understand and to characterize. It can help in developing better quantitative understanding of the operation mechanism of these motors and other similar rotary motors.

Here, we propose a new method of characterizing this feedback. We initially demonstrate experimentally the effect of this feedback on the dynamics of the motor's angular velocity. We then offer a phenomenological model to explain the results obtained, which can be further tested. If confirmed, it can help us in quantitatively measuring the effect of torque on the stator-rotor interaction. The basic idea is that the feedback between torque and stator-rotor interaction can lead to interesting dynamical patterns in the angular velocity of the motor especially under the influence of environmental factors that can contribute to changes in torque. For example, temperature influences the medium's viscosity and the rotational speed, which can change the viscous drag on the motor [15]. In addition, the nano-size structure of these motors and the large number of flexible interacting components they consist of [1,16], make them sensitive to thermal fluctuations. Therefore, we expect that thermal fluctuations would influence the angular velocity of the motor in a frequency-dependent manner. The dependence of the response to thermal fluctuations on frequency, can be used to infer important information about the internal interactions that lead to torque generation in the motor and their dependence on torque.

We have studied the dynamics of the bacterial flagellar motor's angular velocity in response to thermal fluctuations while focusing on the effect of frequency rather than absolute temperature. Our results show that the response of the motor to thermal oscillations with varying frequency, exhibits a resonance at specific frequencies reflecting the rich complex internal dynamics of the motor. These results can be explained with a simple phenomenological model that assumes a negative feedback between the magnitude of the torque generated by the motor and the state of the torque generating units. The results we present here, provide a clear evidence of the importance of studying the dynamics of a rotary motor's angular velocity. They also

demonstrate how these studies can be utilized to infer valuable quantitative information about the interactions between the different components of the motor.

Materials and Methods

Sample preparation. *E. coli* bacteria VH1, expressing yellow fluorescent protein (YFP) were grown at 30°C in 5 mL M9CG [15] while shaking at 240 rpm until early exponential phase ($O.D._{600nm}$=0.1). Cells were centrifuged at 10,000 rpm for 5 minutes and resuspended in 2 mL tethering buffer (10 mM Potassium Phosphate, 0.1 mM EDTA, 67 mM Sodium Chloride, 1 μM L-methionine, and 50 mM glycerol, pH=7) [17]. The harvested cells were then sheared and loaded into channels formed by a microscope glass slide and a cover slip separated by two parafilm straps and left to tether to the surface. Unattached cells were then removed by flushing with tethering buffer, and measurements were carried out as described below.

Experimental Procedure. The microscope slide containing the tethered bacteria was mounted on an inverted microscope (Zeiss, Axiovert 40 CFL). Heating was applied by focusing an infrared laser (λ=1480 nm) through a 20X objective into the sample, and the temperature was changed by changing the laser power through the applied current using a custom written Labview program as depicted in Figure 1A. The rotation of tethered bacteria (depicted in Figure 1B top frame) was observed with 100X objective via fluorescence microscopy, and movies were recorded using a CCD camera (Jenoptik, ProgRes MF) at a rate of 20 fps. The sample temperature around the tethered bacteria was measured using the temperature sensitive dye BCECF, whose fluorescence decreased with temperature as can be seen in the bottom frame of Figure 1B. In all experiments, the laser power was turned on 10 seconds after the recording of the tethered bacterium started and turned of 10 seconds before the recording has ended. During the measurements the laser power was varied by modulating the applied current (see Supplemental Material at [URL] for an example movie depicting the experimental procedure and measurements of temperature and bacterial angular velocity).

Angular velocity measurements. The videos of rotating tethered cells were recorded at 20 Hz in fluorescence mode (see Supplemental Material at [URL] for a movie of the rotating tethered cell in the upper right panel). The location of the cell in each frame was obtained with ImageJ particle analyzer, and that information was used to calculate the angular velocity of the cell using

custom Matlab scripts (Mathworks). The angular velocity of each bacterium was corrected to account for any decrease caused by damage due to the mercury lamp used for fluorescence imaging. Note that the change in the average angular velocity of a bacterium during a single measurement was ~0.2% s^{-1}. The correction comprised of detrending the traces by removing from each trace a linear fit to the average angular velocity including the 10 second steady-state ends of each measurement. The detrended traces from all bacteria measured were then averaged together.

The amplitude of the angular velocity oscillations was calculated for each run, by fitting the angular velocity oscillations to the sin function: $\omega(t) = \omega_0 + \omega_{amp}\sin(2\pi f t)$, where ω_0 is the average angular velocity or steady-state velocity of the motor, ω_{amp} is the amplitude of the angular velocity oscillations, and f is the frequency of the angular velocity oscillations, which is set to be the same as that of the applied temperature oscillations.

Results

Response to thermal oscillations. Our experiments were performed using the mutant *E. coli* strain VH1 [18], with all receptors and chemotactic genes deleted including the response regulator CheY. This allows the flagellar motors to rotate in one direction only. The cells were tethered to the glass surface via their truncated flagella, and their surrounding temperature was changed in a well-controlled manner as described earlier in Materials and Methods. The tethered bacteria were subjected to temperature oscillations around an average background temperature of 31°C, while their angular velocity in response to the thermal oscillations was measured.

As expected, the angular velocity of the motors oscillated with the temperature and at the same frequency. We found, however, that the amplitude of the angular velocity oscillations strongly depends on the frequency of the thermal oscillations. Our results show that the amplitude of the angular velocity oscillations initially increases with the frequency of the thermal oscillations up to a critical frequency around 4Hz, and decreases for higher frequencies, i.e. exhibits resonance around 4Hz. Furthermore, the resonance frequency does neither vary between cells nor as a function of the temperature oscillations amplitude (Fig. 2). Note that for each temperature amplitude in Fig. 2, the angular velocity amplitudes measured for the different frequencies were normalized by the maximal measured amplitude for that temperature. This is to emphasize that the resonance frequency does not change with the amplitude of the temperature

oscillations, and that the relative change between the different frequencies is similar. Note as well, that the amplitude of the temperature oscillations did not change with the frequency (Fig. 1E) as exhibited by the motor's speed. Finally, the presence of the resonance was further verified. This was achieved by combining all the data obtained from different cells and different amplitudes of thermal oscillations together, by averaging the relative change in the amplitude of the angular velocity oscillations measured at the same frequency. Our results, presented in Fig. 3A, show that indeed the resonance is not a noise effect, nor is it an anomaly in individual bacteria.

This resonance we observe in the response of the angular velocity to temperature oscillations is not due to the torsional force resulting from the twisting elasticity of the flagellum [19]. The twisting of the flagella can lead to torsional modes of oscillations that will appear in the rotation of the cell body. The low Reynolds number and heavy load conditions however, under which the experiments were carried out, make this effect negligible. Previous studies have shown that under heavy load conditions, the change in the motor's speed in response to thermal changes is due mainly to changes in the medium's viscosity [20], which indicate that twisting elasticity does not contribute to changes in the motor's rotational speed. The change in medium's viscosity is instantaneous and therefore the speed follows the thermal changes in a similar fashion. This can also be seen from the results presented in Fig. 4; the response of the motor's angular velocity to fast temperature changes applied as a pulse is similar to the motor's response to slow linear changes and exhibits linear dependence on temperature. In addition, the net change in the motor's speed is also similar for the different rates of temperature increase and decrease. Note however, that in these measurements, the temperature was held constant for 10 seconds following any change, allowing the motors to reach steady state. Thus, this resonance cannot be due to the viscosity of the medium either. Even though, changes in the medium's viscosity leads to changes in the motor's angular velocity, the changes in viscosity do not depend on the frequency of temperature oscillations, i.e. does not exhibit resonance.

We conclude that this effect is due to changes in the torque driving the motor's rotation. To verify our conclusion, we have calculated the relative amplitude of the angular velocity oscillations: $\left[\frac{\omega_{max}}{\omega_0}(f)\right] \Big/ \left[\frac{\omega_{max}}{\omega_0}(0.2Hz)\right]$, where $\omega_{max} = \omega_0 + \omega_{amp}$, and ω_{amp}, ω_0, and f are as

defined in Material and Methods. Since $\tau_{max} = \tau_D(T_{max}) \propto \eta(T_{max})\omega_{max}$, (where τ_D is the drag torque on the cell body, η is the medium's viscosity, and T_{max} is the maximal temperature of the thermal oscillation applied, which is the same for all frequencies applied), the measure presented above excludes the effect of viscosity, and is equivalent to the relative maximal magnitude of the torque oscillations: $\tau_{max}(f)/\tau_{max}(0.2Hz)$. Previous studies have argued that temperature itself does not influence the torque, and the change in the angular velocity of the BFM in response to changes in temperature is a result of the change in the medium's viscosity [20]. Therefore, removing the viscosity from the equation, removes as well the effect of temperature. And indeed, as we discussed above the resonance frequency is independent of the amplitude of the thermal oscillations applied (Fig. 2 inset). The division by ω_0, in the expression of the relative amplitude of the angular velocity oscillations, is to account for changes in the angular velocity that might stem from damage caused to the cell over long time between the different measurements. The results presented in figure 3B show that the behavior observed in the change of the angular velocity is indeed a result of a change in the torque generated by the motor.

This behavior resembles the resonance behavior exhibited by driven damped systems with a natural mode of oscillations. Our results can be well-described by the same equation used to describe the oscillation's amplitude of a driven damped harmonic oscillator as a function of the driving-force frequency:

$$Amp(f) = \frac{A_1}{\sqrt{\left(f^2 - {f_0}^2\right)^2 + \gamma^2 f^2}} + A_0 \,, \qquad (1)$$

where f is the driving force frequency, f_0 (= 3.7228 ± 0.25 Hz) is the natural frequency of the system, A_0 is the background noise, and γ is the damping term (Black lines in Fig. 3A and B).

Steady-state fluctuations in angular velocity. The results described above suggest that the BFM has a natural mode of oscillation that affects torque generation. Therefore, it displays a resonance response to an external oscillatory driving force with a frequency similar to the frequency of the natural oscillation. To verify the existence of natural modes of oscillations in the angular velocity of the flagellar motor, we performed spectral analysis of the rotation of

tethered bacteria at steady state. Interestingly, we find that the power-spectrum of the angular velocity of the bacterial flagellar motor measured at steady state conditions at 31°C (Fig. 5A), is very similar to the response curve presented in Fig. 3. It is important to remark here that the resonance frequency is not due to the interaction of the rotating cell body with the surface. The average angular velocity of the bacterium whose spectrum is presented in Fig. 5A is ~2Hz, and in Fig. 3A we present the distribution of the steady state angular velocity of all bacteria measured in our experiments for comparison. In addition, we have measured the power spectrum of the steady-state angular velocity at different temperatures, which changes the average angular velocity. We find that the resonance frequency does not change with either the temperature or the average angular velocity (Fig. 5B and C respectively). This is a further indication, that neither the temperature, nor the average angular velocity is the source of the resonance.

Thus, the natural oscillation must be due to the internal dynamics of the BFM. As mentioned earlier, the BFM consists of a large number of interacting components, whose interactions are dynamic and can exhibit different states with distinct angular velocity. As a result, the angular velocity of the motor will fluctuate between different values. However, random fluctuations do not lead to the rise of natural oscillations. Natural modes of oscillation can appear only when there is a negative feedback mechanism that links the transition rates between the different states and the measured variable [21]. In our case, we have shown that the resonance response is that of the torque generated by the motor (Fig. 3B). This indicates that the torque generated by the motor can influence the rate of transition between the different states of the motor, i.e. larger torque leads to an increase in the transition rate to a state with lower torque and vice versa.

Theoretical Model. The results described above, can be explained with a simple phenomenological model that can account for the measured power spectrum (Fig. 5) and the resonance observed in the response to thermal oscillations (Fig. 3). The model assumes a negative feedback between the torque generated by the motor and the interaction of the torque generating units with the rotor. In detail, the interaction between the torque generating units and the rotor can be in one of two states, active or inactive, and the rates of transition between the two is torque dependent (Fig. 6). Sudden increase in torque amplitude would reduce the number

of active units and vice versa. Thus, the probability of the torque generating proteins to be in the active state P_A is described by:

$$\frac{dP_A}{dt} = -\alpha(\tau)P_A + \beta(\tau)(1 - P_A) + \xi(T)\,, \tag{2}$$

Where ξ is the noise term, T is the temperature, and α and β are the rates of transition between the two different states (active and inactive) which depend on the torque τ. In order to explain the presence of natural modes, the dependence of β and α on τ should be such that α increases as τ increases, while β should increase as τ decreases. As a result, the steady-state probability function $P_A^S = \frac{\beta}{\alpha+\beta}$ would decrease with τ, which would provide the negative feedback required for sustaining an oscillation. Note that this is not inconsistent with the findings of Lele et al [14], since P_A determines the fraction of stators engaged in the motor and not the number of stators in the motor. The two states, active and inactive, can be attributed to the conformation of the rotor proteins FliG, for example, as discussed later. Once a unit is engaged and is generating torque (in the active state) the total torque of the motor will change. The rate of change in the torque around the steady-state torque ($\tau_S = NP_A\tau_0$, where N is the number of torque generating units in the motor, and τ_0 is the torque generated by a single unit) and in first order approximation in τ is given by:

$$\frac{d\tau}{dt} = -\frac{\tau - NP_A(\tau)\tau_0}{t_0}, \tag{3}$$

where, t_0 is the relaxation time to steady-state, which is not the relaxation due to the external drag force (which we assume happens instantly due to the low Reynolds number conditions). t_0 is rather the relaxation of the torque generating units inside the motor. The steady-state torque is taken to be linearly proportional to the number of engaged stators units based on previous measurements [22]. Note that the number of stators in the motor N is assumed to be constant here. The change in the torque magnitude occurs only due to the fluctuations in the number of stators engaged and not by adding or removing stators to and from the motor as in the case of

[14]. Equation (3) then indicates that the torque cannot increase beyond what the engaged stators can provide.

Developing equations 2 and 3 together for small fluctuations around the steady state, where $\tau = \tau_S + \Delta\tau$, and $P_A = P_A^S + p_A$ (see also similar treatment of voltage fluctuations as a result of voltage-gated ion-channels fluctuations between open and closed states [21]), we get the second order differential equation for torque fluctuations:

$$\frac{d^2\Delta\tau}{dt^2} = -\gamma\frac{d\Delta\tau}{dt} - \omega_0^2\Delta\tau + R(T)\,, \tag{4}$$

where $\gamma = \lambda(\tau_S) + \frac{1}{t_0}$, $\omega_0^2 = {}^{\lambda(\tau_S)}/_{t_0} + \lambda_{,\tau}^S P_A^S - \beta_{,\tau}^S = {f_0}^2$, $\lambda = \alpha + \beta$, $\lambda_{,\tau}^S$ and $\beta_{,\tau}^S$ are the derivatives of λ and β at the steady-state torque τ_S respectively, and $R(T) = \frac{N\tau_0}{t_0}\xi(T)$, which will result in $A_1 = \sqrt{|R_\omega|^2}$ (see equation (1)), where $|R_\omega|^2$ is the spectrum of $R(T)$. $\Delta\tau$ here, represent the fluctuations in the magnitude of the torque generated by the motor. The reason thermal oscillations can enhance these fluctuations, is because fluctuations in torque lead to fluctuations in the angular velocity of the motor. If these fluctuations have a natural mode of oscillation, then they will be amplified when the angular velocity is driven by an external perturbation at the natural frequency. In our case, the driving perturbation is applied by temperature. This result provides a direct quantitative link between the internal dynamics of the motor and the measurable parameters of the angular velocity's spectrum. Therefore, it can be used to gain important information about the energy landscape of the motor's internal interactions responsible for torque generation. In order to obtain quantitative information about the transition rates, we need to determine the dissipation constant γ. For that reason we need to measure the change in $\Delta\tau$, rather than the relative change in τ_{max}, which we currently have (Fig. 3B). This requires determining τ_s as $\Delta\tau = \tau - \tau_s$. Thus, more accurate measurements are required, in which the steady-state torque can be determined and controlled. This can be achieved, for example, by changing the size of the object being rotated by the motor. Note however, that current estimations of the relaxation time of the motor upon an increase or decrease in the torque, indicate that t_0 is on the order of second [23]. On the other hand, the

dissipation constant γ, obtained from the best fit to the data, is ~2 s^{-1}. This result stands in good agreement with the existing estimates of t_0 and λ as we will discuss further below.

Discussion and Summary

The description we provide here is phenomenological at this stage. The source of coupling between the torque generated by the motor and the transition dynamics between the different states is still unknown. However, this model explains how such coupling can lead to the resonance described above. Previous studies have shown that such mechanisms do exist. The number of stators in the motor for example was found to increase with the load, which is equivalent to the torque generated by the motor [14,23]. The time scale over which the number of engaged stators change in response to change in the load is much longer than the period of the observed oscillations here. Nonetheless, other coupling mechanisms have been proposed, which occur over comparable time scales to the ones measured here. The dynamics of rotational direction switching was found to depend on the torque generated by the motor [14]. It was shown for example that a mutant strain of bacteria lacking the CheY protein switches its rotational direction under high pressure [24]. Another study have shown that the switching rate of the motor from CCW-to-CW and vice versa increases with the magnitude of the torque generated by the motor [25]. This is in fact the type of negative feedback required for the presence of natural oscillations. Several theoretical models describing the dynamics of the BFM and its switching used this coupling mechanism and negative feedback between switching regulation and torque generation in order to explain observed measurements [26,27]. In all these studies, the basic assumption is that the conformation of FliG proteins can switch between two states which promote rotation in the CW or CCW direction. The role of CheY-P binding to the rotor is to stabilize the switch. In our experiments, CheY is deleted and therefore the motor cannot complete a switching event. However, the FliG proteins can still fluctuate between different states. These fluctuations can change the number of engaged stators driving the rotation of the motor and hence the torque generated by the motor and its angular velocity. If indeed the rates of FliG transition between its different states that promote stator engagement and disengagement, are torque dependent, that would provide the negative feedback required for the appearance of natural modes of oscillations in the torque magnitude. As a result, the response of the motor's angular velocity to thermal fluctuations will exhibit resonance as we demonstrated

here for the first time. Our estimation of λ, which represent the switching rate between the two states of the stators units, agrees well with previous measurements of the CCW-to-CW switching rate. This further supports the hypothesis, that the FliG fluctuations are the source of rotational direction switching, which is stabilized by the binding of CheY-P.

Natural modes of oscillations have been reported before [28], and numerous sources, in addition to the one mentioned above, can account for them as have been postulated previously: a) Fluctuations in the number of engaged stators which will lead to a change in the rotational speed [29]. b) Membrane potential fluctuations caused by changes in internal and external pH as well as membrane conductivity, capacitance or protons import and export activity. We have recently reported a change in the internal pH of bacteria, which is dependent on the chemical environment as well as temperature [15]. c) The friction resisting the rotation of the rotor caused by the interactions between different components of the motor can be another source of speed modulation. Conformational changes of proteins composing the motor can lead to changes in the friction and hence the rotational speed of the motor. d) Recently, it was shown that bacteria can also fine-tune their swimming speed with the help of a molecular brake (YcgR). Upon binding of YcgR to the nucleotide second messenger cyclic di-GMP, it interacts with the motor to curb flagellar motor rotation [30,31]. Even though activation of this network and the resulting deceleration is suggested to coincide with nutrient depletion, it still could have a minor effect on the motor's speed under different conditions. Therefore, changes in the level of interaction between YcgR and the motor, or the concentration of cellular di-GMP can cause fluctuations in the motor's speed.

All the above mentioned factors can cause changes in the torque generated by the motor. However, it is not clear yet, which will result in a natural mode of oscillation since as mentioned earlier, random fluctuations in the torque generation without a negative feedback mechanism cannot lead to natural modes. The experimental technique presented here can be useful for examining the effect of each of the factors discussed above, on the angular velocity of the BFM, and identifying the source of the feedback mechanism that produces the observed natural mode. In addition, this technique can be used to investigate the internal dynamics of biological motors in general and quantitatively determine the interactions between the different components responsible for torque generation.

Acknowledgements: This study was supported in part by the National Science Foundation (Grant PHY-1401576).

References:

[1] Y. Sowa and R. M. Berry, Q. Rev. Biophys. **41**, 103 (2008).
[2] D. White, *The Physiology and Biochemistry of Prokaryotes*, 1st ed. (Oxford University Press, New York, 1995).
[3] Y. Sowa, A. D. Rowe, M. C. Leake, T. Yakushi, M. Homma, A. Ishijima, and R. M. Berry, Nature **437**, 916 (2005).
[4] C. V Gabel and H. C. Berg, Proc. Natl. Acad. Sci. U. S. A. **100**, 8748 (2003).
[5] Y. Asai, S. Kojima, H. Kato, N. Nishioka, I. Kawagishi, and M. Homma, J. Bacteriol. **179**, 5104 (1997).
[6] D. F. Blair and H. C. Berg, Cell **60**, 439 (1990).
[7] R. Mot and J. Vanderleyden, Mol. Microbiol. **12**, 333 (1994).
[8] K. Sato, J. Biol. Chem. **275**, 5718 (2000).
[9] S. Lloyd, H. Tang, X. Wang, S. Billings, and D. Blair, J. Bacteriol. **178**, 223 (1996).
[10] J. Zhou and D. F. Blair, J. Mol. Biol. **273**, 428 (1997).
[11] A. G. Garza, Proc. Natl. Acad. Sci. **92**, 1970 (1995).
[12] J. Zhou, S. A. Lloyd, and D. F. Blair, Proc. Natl. Acad. Sci. **95**, 6436 (1998).
[13] K. K. Mandadapu, J. A. Nirody, R. M. Berry, and G. Oster, (2015).
[14] P. P. Lele, B. G. Hosu, and H. C. Berg, Proc. Natl. Acad. Sci. U. S. A. **110**, 11839 (2013).
[15] M. Demir and H. Salman, Biophys. J. **103**, 1683 (2012).
[16] H. C. Berg, Annu. Rev. Biochem. **72**, 19 (2003).
[17] E. Paster and W. S. Ryu, Proc. Natl. Acad. Sci. U. S. A. **105**, 5373 (2008).
[18] R. G. Endres, O. Oleksiuk, C. H. Hansen, Y. Meir, V. Sourjik, and N. S. Wingreen, Mol. Syst. Biol. **4**, 211 (2008).
[19] S. M. Block, D. F. Blair, and H. C. Berg, Nature **338**, 514 (1989).
[20] J. Yuan and H. C. Berg, Biophys. J. **98**, 2121 (2010).
[21] H. Salman, Y. Soen, and E. Braun, Phys. Rev. Lett. **77**, 4458 (1996).
[22] S. W. Reid, M. C. Leake, J. H. Chandler, C.-J. Lo, J. P. Armitage, and R. M. Berry, Proc. Natl. Acad. Sci. U. S. A. **103**, 8066 (2006).
[23] M. J. Tipping, B. C. Steel, N. J. Delalez, R. M. Berry, and J. P. Armitage, Mol. Microbiol. **87**, 338 (2013).
[24] M. Nishiyama, Y. Sowa, Y. Kimura, M. Homma, A. Ishijima, and M. Terazima, J. Bacteriol. **195**, 1809 (2013).
[25] J. Yuan, K. A. Fahrner, and H. C. Berg, J. Mol. Biol. **390**, 394 (2009).
[26] F. Bai, T. Minamino, Z. Wu, K. Namba, and J. Xing, Phys. Rev. Lett. **108**, 178105 (2012).
[27] G. Meacci, G. Lan, and Y. Tu, Biophys. J. **100**, 1986 (2011).
[28] M. Kara-lvanov, M. Eisenbach, and S. R. Caplan, Biophys. J. **69**, 250 (1995).
[29] G. Meacci and Y. Tu, Proc. Natl. Acad. Sci. U. S. A. **106**, 3746 (2009).
[30] K. Paul, V. Nieto, W. C. Carlquist, D. F. Blair, and R. M. Harshey, Mol. Cell **38**, 128 (2010).
[31] A. Boehm, M. Kaiser, H. Li, C. Spangler, C. A. Kasper, M. Ackermann, V. Kaever, V. Sourjik, V. Roth, and U. Jenal, Cell **141**, 107 (2010).

Figures

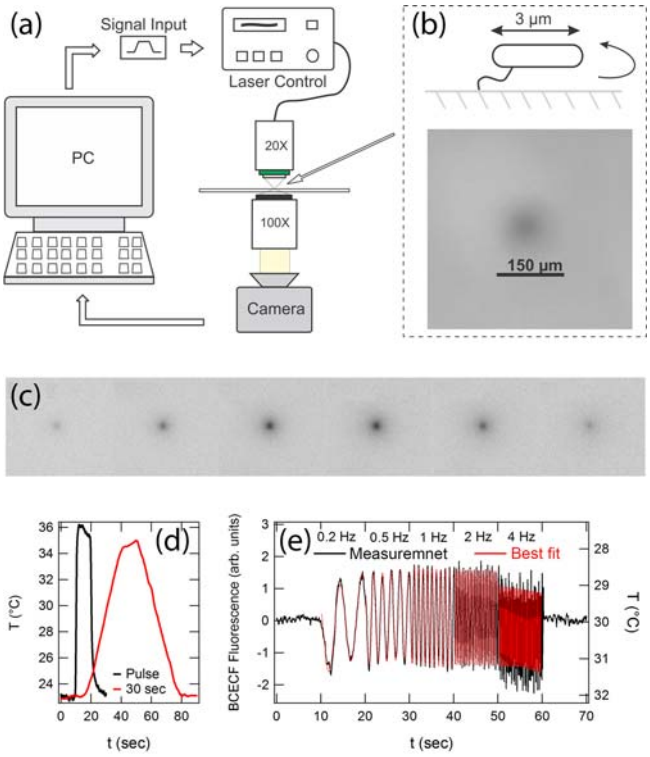

Fig. 1. Experimental procedure. The experimental setup used for temperature modulation and recording of tethered cells' rotation is presented in (a). The infrared laser was focused into the sample and its power was controlled via a custom written Labview program. The temperature around the tethered bacteria (presented in the top frame of (b)) was measured using the temperature sensitive dye BCECF as can be seen in the bottom frame of (b) and the time series presented in (c). Examples of the temperature measurements as a function of time using this method for linear and oscillatory change in temperature are presented in (d) and (e) respectively. The different lines in (e) represent the actual temperature measurement, which is noisy, and the best fit to a sinusoidal curve as indicated in the figure legend. Observations were made on an inverted microscope in fluorescence mode with a 100x objective. The tethered cells' rotation was recorded using a CCD camera. For more information, see Supplemental Material at [URL].

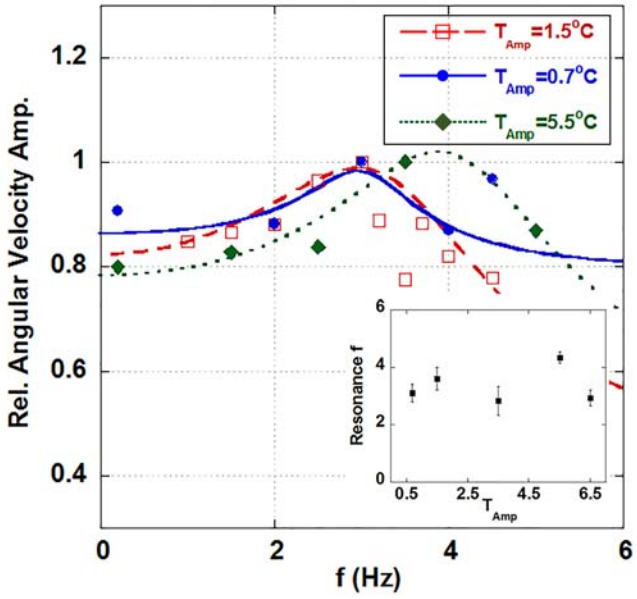

Fig. 2. The effect of temperature oscillations' amplitude on the resonance frequency. The position of the resonance (resonance frequency) and the relative change in the amplitude of the angular velocity oscillations do not depend on the amplitude of the temperature oscillations. We have changed the amplitude of the temperature oscillations around the 31°C, from 0.7°C to 6.5°C. The data points in the main figure depict the relative change in the angular speed oscillations amplitude as a function of the temperature oscillations frequency. The different shapes depict different temperature oscillations amplitude as indicated in the legends. Each data point is the average of at least 30 measurements. Resonance frequencies for all amplitudes of temperature oscillations were obtained by fitting the data to the resonance equation (equation (1) in the text). The fits are depicted by the lines in the figure. Resonance frequencies as a function of the temperature oscillations amplitude are presented in the inset. The error bars depict the fit errors. Our findings also found the relative change in the oscillations' amplitude of the angular velocity to be similar.

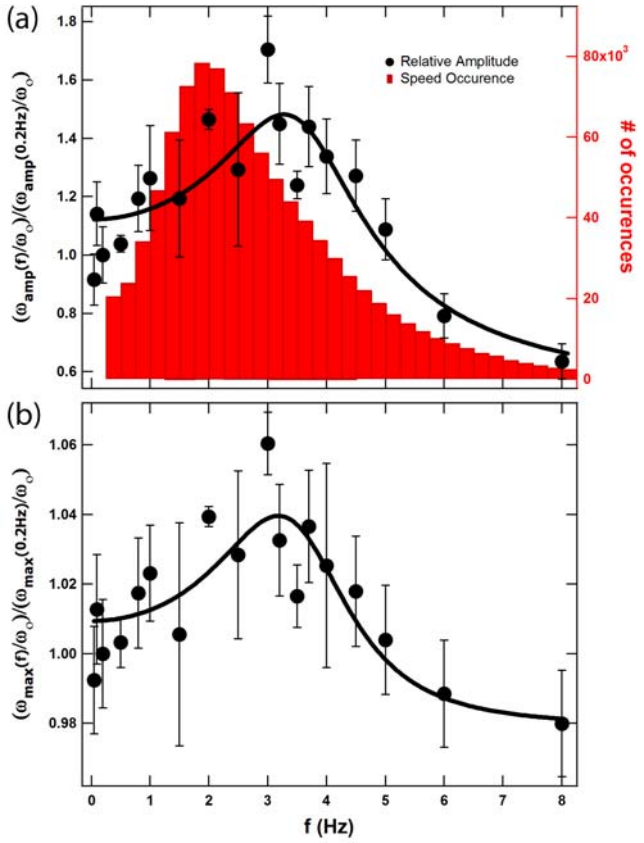

Fig. 3. The oscillations' amplitudes the motor's angular velocity and torque in response to temperature oscillations. (a) The Relative amplitude ($\frac{\omega_{amp}(f)}{\omega_0} \Big/ \frac{\omega_{amp}(0.2Hz)}{\omega_0}$) of the angular velocity oscillations was calculated as described in Materials and Methods. Relative amplitudes of a single experiment set were normalized with the relative amplitude at 0.2 Hz, and the normalized relative amplitudes are averaged for all experiments. The average normalized relative amplitude increases as the oscillation frequency increases up to 3-4 Hz and decreases sharply above resonance frequency (circles). The line is the best fit to the equation in the text. Comparison with the speed histogram (bars) confirms that bacterium-surface hydrodynamic interactions is not the cause of the observed resonance. (b) The relative maximal torque magnitude calculated from the ratio of the relative speed as described in the main text, which eliminates the effect of viscosity changes due to temperature as explained in the text. Each data

point in the figure was obtained by averaging at least 30 different measurements from several different bacteria. The error bars depict the standard deviation of the different measurements.

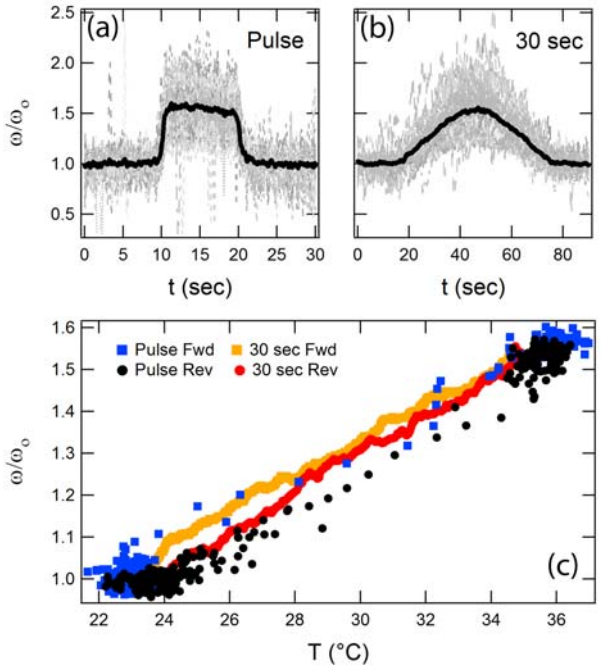

Fig. 4. The response of the bacterial flagellar motor's speed to linear change in temperature. The motor's relative rotational speed as a function of time in response to linear temperature change applied at different rate is presented in (a) (The laser was applied as a pulse) and (b) (the laser power was increased over a period of 30 seconds). Grey dashed lines depict the rotational speed of different bacteria. Black thick lines depict the averages of each set of experiments. The speed was normalized by its value at room temperature. The number of bacteria recorded for temperature increases as a pulse and over the period of 30 seconds are 46, and 54 respectively. (c) The average relative speed is presented as a function of temperature for both modes of temperature increase. Note that the change in speed is almost linear with temperature in both cases and no deference is detected within our error estimate.

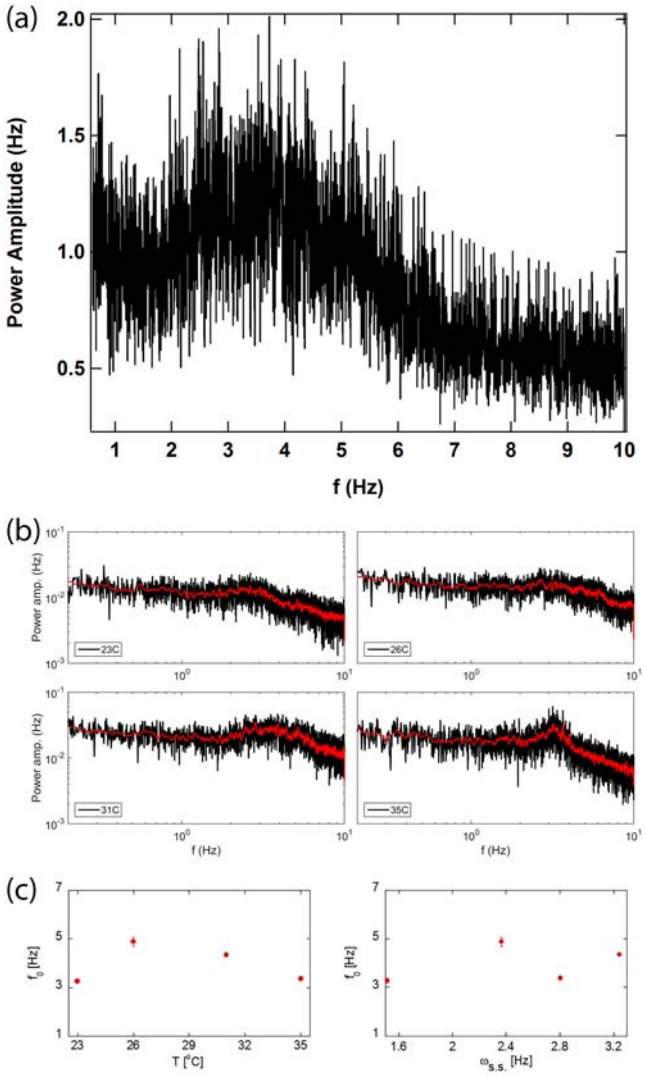

Fig. 5. Spectral analysis of the bacterial rotational speed at steady state. The Power spectrum density functions of a tethered bacterium recorded for ~3 minutes at a 30 frames/second are presented. In (a) the measurement was done at 31°C, and as clearly evident, the rotational speed exhibits a natural mode of oscillation at the same frequency where the resonance was observed in Fig.3, even though the rotational speed of this bacterium was ~2Hz. The power spectrum density function was measured for the several bacteria at different temperatures as well, as indicated in each panel of (b). Note that, the position of the resonance does not seem to depend on temperature or steady-state angular velocity, and appear to fluctuate around 4Hz. It is though more pronounced for higher temperature. (c) The resonance frequency obtained by fitting the spectra in (b) to the resonance equation (equation (1) in the text) is plotted as a function of

temperature (left) and average steady-state angular frequency (right). The error bars depict the fit error.

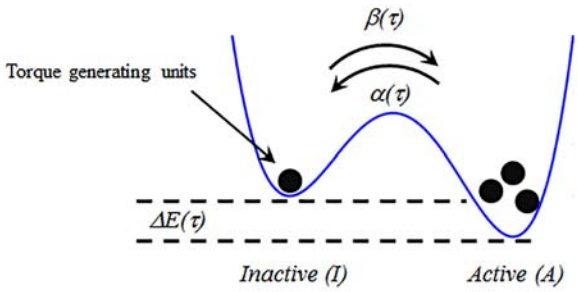

Fig. 6. A Phenomenological Model. The torque generating units in the motor can be in one of two states, active and inactive or engaged and unengaged. The transition between the two states depends on the torque being generated by the motor at the time of transition.